UNIVERSITY OF CALIFORNIA, MERCED

DELIVERY OF ANTI-INFLAMMATORY PROTEINS ACROSS THE HUMAN BLOOD BRAIN BARRIER FOR THE TREATMENT OF TRAUMATIC BRAIN INJURY AND RELATED PATHOLOGIES

A Thesis submitted in partial satisfaction of the requirements for the degree of Master of Science

in

Chemistry and Chemical Biology

by

Loan Nguyen

Committee in charge:
Dr. Mathew Meyer, Chair
Dr. Patricia LiWang, Advisor
Dr. Andy LiWang
Dr. Masashi Kitazawa

2016

Thesis of Loan Nguyen is approved, and it is acceptable in quality and form for publication on microfilm and electronically:

_____	
Professor Mathew Meyer (Chair)	Chemistry and Chemical Biology
_____	
Professor Patricia LiWang	Chemistry and Chemical Biology
_____	
Professor Andy LiWang	Chemistry and Chemical Biology
_____	
Professor Masashi Kitazawa	Department of Medicine, University Of California, Irvine

ABSTRACT
DELIVERY OF ANTI-INFLAMMATORY PROTEINS ACROSS THE HUMAN BLOOD BRAIN BARRIER FOR THE TREATMENT OF TRAUMATIC BRAIN INJURY AND RELATED PATHOLOGIES

Traumatic Brain Injury (TBI) is an injury that occurs following sudden head trauma and results in extensive damage to brain tissue primarily due to the acute inflammatory response. However, current treatment options for TBI are limited due to the difficulty in delivering therapeutic agents to the brain. The severity and consequences of pathologies directly and indirectly associated with TBI have attracted significant medical attention and have stimulated research directed at finding new therapeutic options for the treatment of the inflammation that accompanies TBI. Many studies have identified the crucial role of chemokines and chemokine receptors in triggering and perpetuating this inflammatory response. This study reports a potent drug target for combatting TBI induced inflammation, which is constructed by conjugating the chemokine antagonist, vMIP-II and the single chain variable fragment, scFv8D3, of the antibody that selectively binds to Transferrin receptors expressed on the external side of the human blood brain barrier (BBB). Combining the functionality of these well-studied anti-inflammatory and transport-oriented proteins would greatly facilitate the delivery of therapeutic agents to the brain. The chimeric protein vMIP-II-L-scFv was successfully designed, expressed in an *E. Coli* system and refolded using stepwise dialysis with different concentrations of Gnd-HCl, Arginine-HCl, and oxidizing agent GSSG, providing a solid platform for the investigation of its BBB transport and anti-inflammatory properties in future studies.

Loan Nguyen

December 2016

ACKNOWLEDGMENTS

I would like to express my deepest appreciation to my advisor, Dr. Patricia LiWang, for her endless guidance, patience and moral support. She has generously given her time to discuss and troubleshoot any problems during my project and has provided opportunities to learn and to improve my problem-solving skills. I also would like to thank Dr. Li Zhang and Dr. YongGang Chang for their scientific insights, training, and help throughout my graduate research. I also want to thank Dr. YongGang Chang for his time and patience when he trained me in NMR spectroscopy and protein purification techniques. I would like to thank Dr. Archana Chavan for her friendship and moral support during my emotional journey for the past years. I also appreciated the assistance and support from Megan Schill who has spent countless nights working on this project with me and all the LiWang lab members for all of the enjoyable conversations and company they have provided.

Finally, I would like to thank loving parents and siblings who have always stand by me and never lost faith in me even when I was the most frustrated and unreasonable. Thank you for keeping me sane and happy everyday.

NOMENCLATURE

ABTS= 2,2'-azino-bis(3-ethylbenzothiazoline-6-sulphonic acid)

βME= beta mercaptoethanol

EDTA= Ethylenediaminetetraacetic Acid

ELISA= enzyme-linked immunosorbent assay

IPTG= Isopropyl b-D-1-Thiogalactopyranoside

Gnd-HCl= Guanidine Hydrochloride

GSSG= Glutathione disulfide (oxidized form)

His-tag= Hexahistidine Tag

LB= Luria Broth

NaCl= Sodium Chloride

NaPi=Sodium Phosphate

Ni-NTA= Ni-conjugated chromatography beads, using NTA (nitrilotriacetic acid) to chelate the Ni^{+2} ions. This "nickel column" binds tightly to poly-histidine segments in protein and is used for affinity purification.

O.D= Optical Density; TCA, trichloroacetic acid

SDS-PAGE, Sodium Dodecyl Sulfate Polyacrylamide Gel Electrophoresis

scFv8D3= singe chain variable fragment of antibody 8D3. In this work, there is a 20 a amino acid linker between the variable light and variable heavy region of the protein.

Sumo =N-terminal SUMO fusion tag

SumovL10s=Sumo-vMIP-II linked to scFv8D3 with 10 Glycine and Serine linkers

Txn-scFv8D3= N-terminal Thioredoxin fusion tag linked to scFv8D3

TABLE OF CONTENTS **Page**

LIST OF FIGURES **Page**

CHAPTER 1: INTRODUCTION: THE CHALLENGE TO TREAT TRAUMATIC BRAIN INJURY

The brain is one of the most complex and important organs in humans due to its integral role in regulating the function of every organ in the human body and controlling all aspects of life in an individual such as recognition, personality and motor activities. Damage to the brain leads to many serious consequences in a person's life, and traumatic brain injury is one of the most common causes of damage to the brain.[1,2] Most people are at risk of sustaining a traumatic brain injury due to the prevalence of TBI arising from common accidents, such as a person falling and hitting their head on a hard object or being involved in a car accident. Soldiers who are actively serving in war zones often have a higher risk of suffering from TBI.[1] According to the Centers for Disease Control and Prevention, Traumatic brain injury (TBI) is a major cause of death and disability in the United States, contributing to about 30% of all injury deaths. Every day, 138 people in the United States die from injuries that involving TBI.[1] Moreover, there is a close association of TBI with other diseases involving neural inflammation and degeneration.[2] TBI not only causes severe physical damage to the patient but also imposes extensive emotional and financial burdens on their family members. These types of injuries have garnered increasing attention from medical researchers and the public as TBI can lead to various disabilities such as difficulties in recognition, memory loss and sudden personality changes in people who suffer from this condition. Research studies focused on the mechanisms involved in TBI have identified a strong association between brain damage and inflammation.[2] Thus, current therapeutic strategies have focused on finding

the drug targets that inhibit brain inflammation in the hope of preventing TBI-related brain damage. Unfortunately, most drugs cannot be delivered to the injured area in the brain to counteract the inflammatory response due to the high selectivity of the blood brain barrier (BBB).[3] The BBB is structurally formed by the tight junctions between adjacent microvascular endothelial cells and regulates the entry of molecules to the brain from the circulating blood, serving as a defense mechanism to protect the brain from external toxins. Only lipid-soluble molecules under a threshold of 400–600 Da are able penetrate this protective layer, whereas most large molecular weight drugs including peptides, recombinant proteins, monoclonal antibodies, gene therapies do not cross the BBB.[3,4] This reveals the ultimate challenge for the effective treatment of TBI as finding a method which allows anti-inflammatory drugs to successfully pass the BBB and inhibit brain inflammation.

The causes of brain inflammation have been studied intensively in order to find the optimal target for anti-inflammatory treatments. Chemokines and chemokine receptors were found to play a crucial role in the activation and migration of immune cells to the injured site of the brain after traumatic brain injury causing an inflammatory immune response.[5,6] Chemokines are small-secreted proteins which act as chemoattractants of various immune cells such as macrophages and neutrophils and induce their migration to the site of infection or injury. The binding of a chemokine to chemokine receptors on the cell surface triggers the signaling cascade resulting in the infiltration of leukocytes and subsequent inflammation in the brain.[5,6,7] Hence, inhibiting the binding of chemokines to their receptors at the injured sites presents a promising therapeutic target for reducing acute inflammation resulting from injury as well as

chronic inflammation caused by other inflammatory diseases. The viral macrophage inflammatory protein-II (vMIP-II) encoded by the Kaposi's sarcoma associated human herpesvirus 8 is a human chemokine analog that share more than 40% identity to natural human chemokines MIP-1α and MIP-1β, which play a paramount role in the inflammatory immune response.[8,9] vMIP-II can bind to various chemokine receptors CCR5, CXCR4, CCR1, and CCR2 with high affinity, and generally does not induce the pro-inflammatory response mediated by the natural receptor ligands.[9,10] This ability to bind a variety of human chemokine receptors with an affinity comparable to their natural binding partners makes vMIP-II one of the most potent antagonist of the binding of human chemokines to their respective chemokine receptors and therefore makes it a potent inhibitor of the inflammatory response. Thus, engineering a way to deliver vMIP-II across the human BBB to the site of injury in the brain presents a very attractive target for the treatment of TBI.

The human body uses many different pathways to transport specific nutrients, amino acids, and essential metals, such as glucose and iron, from the blood to the brain. One of the most efficient pathways is that used to shuttle iron across the BBB to the brain via transferrin mediated receptor endocytosis.[3,11] Transferrin is the iron bound protein which binds tightly to the transferrin receptors (TfR) that are expressed abundantly on the surface of brain endothelial cells allowing their endocytosis across the BBB.[11] Yu Li's group developed a particular approach which employs this existing pathway for the delivery of biotinylated drugs across the BBB through the use of a fusion protein comprising the single chain of the antigen-binding region (scFv) of mouse-anti-rat transferrin receptor antibody OX26, and streptavidin. This strategy harnesses the high

affinity of OX26 for TfR to cross the barrier, and the high affinity of streptavidin for biotin to carry the biotinylated drug.[12] Therefore, our aim was to develop a feasible, sufficient and non-invasive strategy to suppress brain inflammation using a recombinant protein comprised of the chemokine antagonist, vMIP-II, and specific brain target transportable vector, scFv that will bind the transferrin receptor. The rat anti mouse TfR antibody, 8D3 was chosen for this study and the variable region of the light chain of 8D3, scFv8D3, was conjugated at the C-terminus of vMIP-II using a 10 residues length linker of Glycine and Serine.[13] This fusion protein, vMIP-II-L-scFv8D3 is designed to both transport the vMIP-II across the BBB via TfR-mediated transcytosis and act as the antagonist to chemokines in the brain.

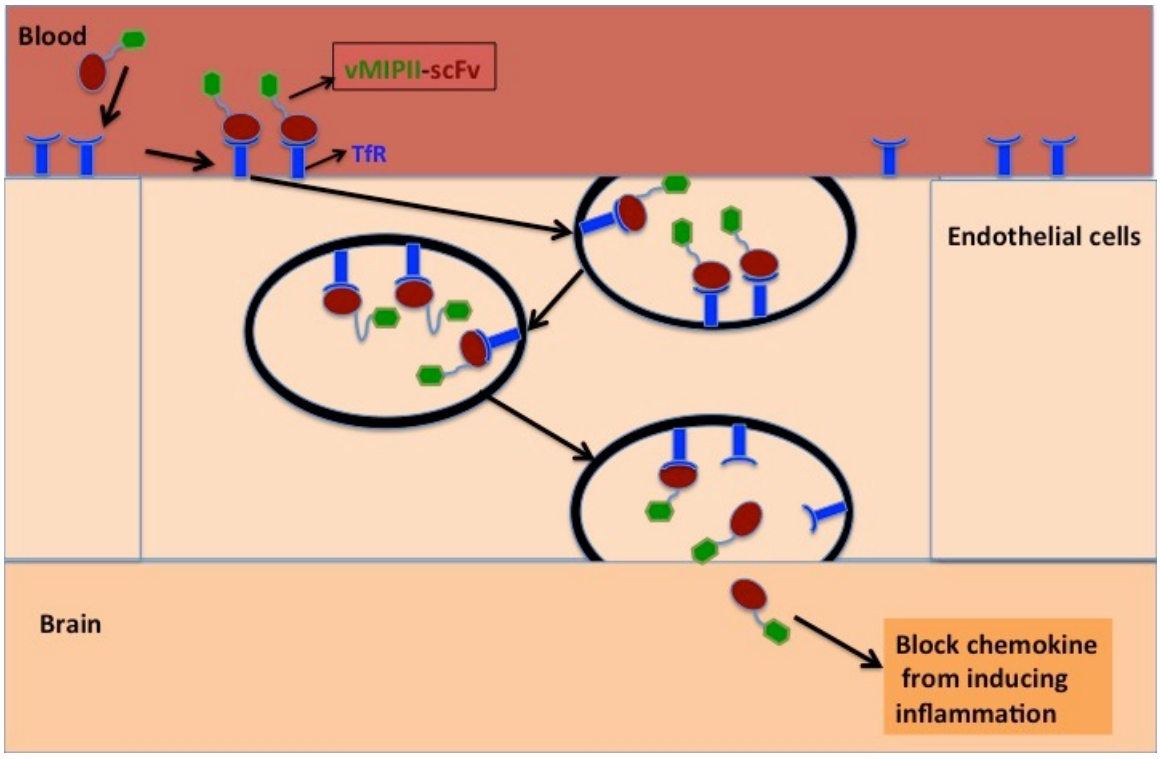

Figure 1: The proposed mechanism of the transcytosis of vMIPII-L-scFv across BBB to suppress inflammation in the brain. The 8D3 scFv recognizes the transferrin receptor TfR and the binding of the scFv to TfR induces the formation of endosomes and allows endocytosis across the BBB. The fusion protein is then released inside the brain where vMIP-II is expected to compete with other chemokines for receptor binding and to reduce the immune signaling causing inflammation.

CHAPTER 2: EXPERIMENTAL PROCEDURES

2.1 Protein Expressions and Purification:

The gene encoding the fusion protein of vMIP-II linked to scFv8D3 with 20 amino acids Glycine –Serine linker was codon-optimized for expression in *Escherichia coli* (*E. Coli*) and purchased from Genescript (Piscataway, NJ) in pUC-57 with various cloning sites. The initial 20 amino acid linker was composed of Glycine and Serine residues with the arrangement of Glycine-Glycine-Glycine-Glycine-Serine $(G_4S)_4$. The gene encoding for linker was selectively designed with non-repeatable codons to allow adjustment of the length of the linker by overlapping extension polymerase chain reactions. However, a longer linker increases the hydrophilicity of the linker leading to a higher chance of aggregations and more difficulty in refolding of the protein. Furthermore, the linker between vMIP-II and scFv8D3 has to maintain the optimal separation between vMIP-II and scFv8D3 to avoid the cross-interaction of vMIP-II to scFv8D3. Therefore, the linker between vMIP-II linked and scFv8D3 was shortened to 10 amino acids (a Gly-Ser residues linker) and the short-linker version is referred to hereafter as vL10. The vL10 gene was cleaved out of the pUC57 plasmid and sub-cloned into pET32a with an N-terminal Thioredoxin fusion tag between NcoI and SalI restriction endonuclease cleavage sites. The vL10 gene was also sub-cloned into the pET28a plasmid using overlapping extension PCR to insert a Sumo fusion tag at the N-terminus. These constructs are referred to as Txn-vL10s and Sumo-vL10s, respectively. As a control for the project, analogous constructs of scFv8D3 without vMIP-II were also made. The gene of Txn-scFv8D3 in pET32a was synthesized using Txn-vL10s as the

template for the PCR. However, cleavage of Txn-scFv8D3 with Enterokinase is required to remove the Txn tag to obtain a native vMIP-II N-terminus, which is necessary for vMIP-II to effectively bind chemokine receptors. One of the disadvantages of a using purification process requiring this step is the slow activity of Enterokinase, as 5-7 days are required for the Enterokinase to completely cleave the Txn fusion tag. In order to avoid this undesirable step, two cleavage sites of the NdeI restriction endonuclease were identified immediately upstream and downstream of the Txn tag located at the N-terminus of the scFv8D3 gene. This design allowed the Txn tag to be removed by single digestion reaction of Txn-scFv8D3 with NdeI leaving only a hexahistidine tag intact at the N-terminus of scFv8D3 ((the construct without a Txn tag is denoted 6xHis-scFv8D3). The gene sequences of all constructs were verified by DNA sequencing service from UC Berkeley to confirm the correct sequences prior to protein expression and purification. [Figure 2b]

The Sumo-vL10-pET28a and 6xHis-scFv8D3-pET32a plasmids were transformed into *E.coli* BL21(DE3) Gold cells. Since each of the plasmids has gene conferring a different antibiotic resistance, appropriate antibiotic was used to grow the transformed cells. 6xHis-scFv8D3-pET32a and Sumo-vL10s-pET28a cells were grown on LB agar plates with the concentration of 100ug/mL ampicillin and 50ug/mL kanamycin, respectively, at 37 °C for 14 hours. For the large scale production of the protein, 20-30 colonies from each LB Agar plate were first inoculated into starter cultures of 5mL LB with either 50 ug/mL kanamycin or 100 ug/mL ampicillin and grown in a shaker at 37 °C, 220 rpm for two hours. The starter cultures were then added into 1 L of M9 minimal medium containing $^{15}NH_4Cl$ as the sole source for Nitrogen with appropriate antibiotics.

The cultures were grown in the shaker at 37 °C and 220 rpm until the cultures reached the OD600 of 0.6-0.8. The protein expression was under the control of a T7 promoter and was induced by the addition of 1 mM IPTG. The cultures were grown at 37°C for 5 hours for 6xHis-scFv8D3 and at 22°C for 16 hours for Sumo-vL10s and shaken at 220 rpm. The cells were harvested by centrifugation at 4200×g at 4 °C for 10 min and the supernatant was discarded. The harvested cell pellets were suspended in 25 mL of 500 mM NaCl and 20 mM Tris (pH 8.0) until a homogeneous cell suspension was obtained. The suspended cells were lysed using an Avestin high-pressure cells homogenizer at 10000psi. The cell lysate was collected on ice to prevent protease activity and then centrifuged at 27,000×g for 1 hour at 4 °C. The supernatant was discarded, and the pellet containing the most of the protein was solubilized in the Resuspension Buffer (6M Guanidinium chloride, 200mM NaCl, 50 mM Tris, 1mM EDTA, pH 8.0) and reduced with addition of 5 mM βME overnight at 4 °C. The protein solution was then centrifuged at 27,000×g for 1 hour at 4 °C to remove the cell debris. The supernatant was further reduced with 5mM βME to make the total of 10mM βME for 3 hours at 4 °C. [Figure 2b]

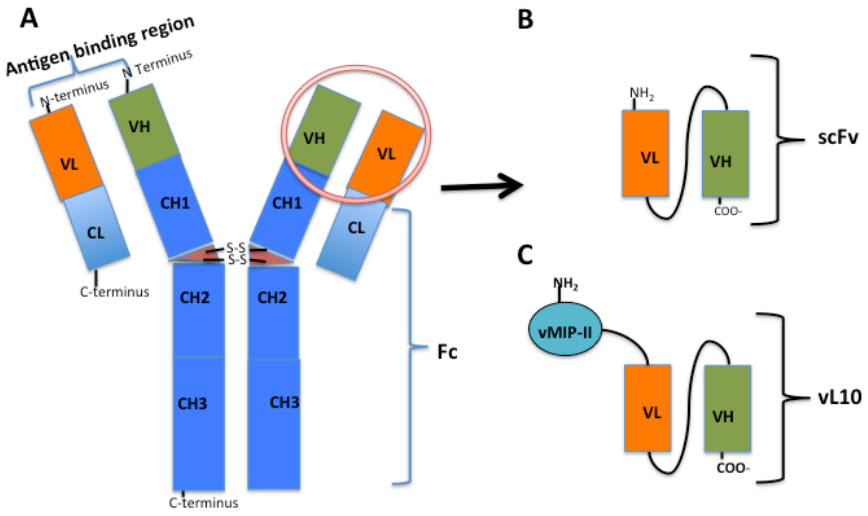

Figure 2: The design of scFv8D3 and vMIP-II-Link-scFv8D3 protein construct.

a. The structure of rat against mouse transferrin receptor antibody, 8D3.

b. The design of scFv8D3: The variable region and the light and heavy chain of a rat against mouse transferrin receptor, 8D3, was conjugated using 20 residues of Gly-Ser linker to connect the two variable chains. c. The overall designed chimeric protein, with N-terminal vMIP-II, followed by a 10 amino acid Gly-Ser linker, then the scFv8D3 as described in (b).

2.2 Refolding of 6xHis-scFv8D3 using Guanidine-HCl gradient Dialysis:

The protein was refolded using a similar approach to the serial dialysis procedures previously described in Umetsu et al.[14] The supernatant was transferred to SpectraPor 3 tubing with a weight cutoff (MWCO) of 3500 Da and dialyzed against 1 L of the same Resuspension Buffer without βME (6 M Guanidinium-chloride, 200mM NaCl, 50 mM Tris, 1mM EDTA, pH=8) to remove the reducing agent for 24 hours at 4 °C. The supernatant was dialyzed against serial dialysis buffers with the same concentration of 200mM NaCl, 50 mM Tris, 1mM EDTA and a decreasing concentration of Guanidine-HCl from 6M to 3 M, 2 M, 1 M, then 0.5 M. These dialysis buffers were referred to as 6 M, 3 M, 2 M, 1 M or 0.5 M Gnd-HCl Buffer. Each dialysis was carried out for 24 hours at 4 °C with minimal stirring. At the 1 M Gnd-HCl Buffer stage, Arginine and oxidizing agent, oxidized glutathione (GSSG), were added into the refolding buffer to make the final concentration of 400 mM Arginine and 375 μM followed the procedure described in Umetsu et al.[14] The 6xHis-scFv-protein solution was dialyzed twice against 1L of 0.5 M Gnd-HCl Buffer to facilitate the formation of correct disulfide bonds in the protein. The

supernatant was then dialyzed 4 times against 1L of Native Buffer (200 mL NaCl, 50 mM Tris, pH=7.5) to remove all the denaturant and additives. The lysate was clarified by centrifugation for 10 minutes at 4000g, 4 °C. Supernatant was loaded onto 3 mL Ni-NTA column equilibrated with Native Buffer (200 mM NaCl, 50 mM Tris, pH 7.5). The Ni column was washed with 15-columns volume of 20mM Imidazole Wash Buffer (200 mM NaCl, 50 mM Imidazole, 20 mM Tris, pH 7.5) and 50 mM Imidazole Wash Buffer (200 mM NaCl, 50 mM Imidazole, 50 mM Tris, pH 7.5). The protein 6xHis-scFv was eluted with Elution Buffer (200 mM NaCl, 250 mM Imidazole, 50 mM Tris, pH 7.5) in 2-3 mL fractions. The fractions containing 6xHis-scFv were identified by SDS-PAGE and the fractions containing the largest amounts of protein were combined and dialyzed against 4 of 1 L of NMR Buffer (100 mM NaCl, 20 mM NaPi, pH=7.5) at 4 °C prior to taking the NMR spectrum to check for the folding of the protein. The absorbance of 6xHis-scFv8D3 was measured at 280 nm and its concentration can be determined using an extinction coefficient of 52620 M^{-1} cm^{-1}.

2.3 Refolding of Sumo-vMIPL10s by Guanidine-HCl gradient dialysis:

The protein was refolded using the serial dialysis procedures similar to the refolding procedure of 6xHis-scFv8D3 and previously described in Umetsu et.al with a few modifications at the 1M Gnd-HCl stage[14]. The cell pellet was resuspended in 6M Gnd-HCl, 200mM NaCl, 50 mM Tris, 1mM EDTA, 10 mM BME, pH 8.0. The protein concentration of Sumo-vL10s was adjusted to 15uM using the Resuspension Buffer and solubilized overnight at 4 °C. An adequate amount of 12.5M βME was added to the supernatant to achieve a final concentration of 10 μM βME. The protein solution was reduced for 3 hours at 4 °C. Similar to the refolding process used for 6xHis-scFv, the

supernatant was transferred to SpectraPor 3 tubing with MWCO of 3500 Da and was first dialyzed against 1 L of 6 M Gnd-HCl Refolding Buffer to remove the βME for 24 hours at 4 °C. The supernatant was then sequentially dialyzed against 1 L each of 3 M, 2 M, 0.5 M and 0.25 M Gnd-HCl refolding buffer for 24 hours at 4 °C. A solubilizing agent (Arginine-HCl) and oxidizing agent (oxidized glutathione, GSSG) were also added into the 1 M, 0.5 M, 0.25 M Refolding Buffers. The supernatant was then dialyzed against 4 of 1L of Ni-NTA column Equilibration Buffer (200mL NaCl, 20mM NaPi, 50 mM Arginine-HCl, 50 μM GSSG, pH 7.5). The lysate was clarified by centrifugation for 10 minutes at 7200g, 4 °C, twice. The supernatant was loaded onto a 3mL Ni-NTA column equilibrated twice to ensure that the protein would bind to the Ni column effectively. The Ni-NTA column was washed with 15-column volumes of 20 mM Imidazole Wash Buffer (200 mM NaCl, 50 mM Imidazole, 20 mM NaPi, pH 7.5) and Wash Buffer 2 (200 mM NaCl, 50 mM Imidazole, 20 mM NaPi, pH 7.5) to remove contaminants, unbound protein and non-specifically bound protein. The protein Sumo-vL10s was eluted with Elution Buffer (200 mM NaCl, 250 mM Imidazole, 20 mM NaPi, pH 7.5) in 3 mL fractions. The fractions containing Sumo-vL10s were identified by SDS-PAGE and combined and dialyzed against 4 of 1 L of Native Buffer (200 mM NaCl, 20 mM NaPi, pH=7.5) at 4 °C to remove the imidazole in the protein solution prior to cleaving the Sumo fusion tag. The buffer was changed every 12 hours. At the third dialysis of Sumo-vL10s in Native Buffer, the Sumo protease ULP-1 (produced in-house) was added into the protein solution at a ratio of 1:200 to remove the Sumo tag. The cleavage of Sumo was allowed to occur at 4 °C overnight. Aggregates formed upon the cleavage of the Sumo solubility tag and were removed by centrifugation for 10 minutes at

7200 g, 4 °C. The refolded protein solution was passed through 3 mL Ni-NTA affinity column that has been equilibrated with 15 column volumes of Native Equilibration Buffer. Upon cleavage by ULP-1, the target protein does not contain a His tag and is eluted out of the column with the flow-through. The flow-through was collected from the Ni-NTA column into a sterile 50 mL tube. The column was then washed with 15 column volumes of Wash Buffer (200 mM NaCl, 20 mM Imidazole, 20 mM NaPi, pH 7.5), and the Sumo tags resulting from the cutting reaction by ULP-1 and the uncut Sumo-vL10s protein were eluted with 25 mL of Elution Buffer (200 mM NaCl, 250 mM Imidazole, 20 mM NaPi, pH 7.5). These wash and final eluted fractions were collected and analyzed using SDS-PAGE to confirm the efficacy of the ULP-cutting reaction and evaluate the purity of the fusion tag free vMIP-II-L-scFv8D3. The fraction containing the cut vL10s was identified using SDS-PAGE. The absorbance of vL10s was measured at 280 nm and its concentration can be determined using an extinction coefficient of 72350 M^{-1} cm^{-1}.

2.4 NMR Spectroscopy:

An NMR sample of 6xHis-scFv8D3 was prepared in a total volume of 350uL at 27uM of 6xHis-scFv8D3 in the buffer of 100mM NaCl, 20 mM NaPi, 5% D2O, 90% H2O and 10 μM DSS of DSS, pH=7.5. The 2D Heteronuclear Single Quantum Coherence (2D-HSQC) experiment was carried out at 25°C, on a 600-MHz Bruker AVANCE III NMR spectrometer with Cryoprobe. The NMR spectrum was acquired with carrier positions of 4.75 ppm for ^{1}H and 119.3 ppm for ^{15}N; sweep widths of 8417.509 Hz (14.0027 ppm) for ^{1}H and 1766.658 Hz (29.0 ppm) for ^{15}N.

NMR spectra of vMIP-II-L-scFv8D3 were acquired from 0.35-ml samples at 10uM in 150mM NaCl, 20 mM NaPi, 10% D2O, 90% H2O and 5uM of DSS, pH=7.5.

All NMR data were collected at 37°C, on a 600-MHz Bruker AVANCE III NMR spectrometer with Cryoprobe. The NMR spectrum was processed at the proton carrier position of 4.75 ppm for ^{1}H and 119.3 ppm for ^{15}N, sweep widths of 8417.509 Hz (14.0027 ppm) for ^{1}H and 1766.658 Hz (29.0 ppm) for ^{15}N.

3. RESULTS AND DISCUSSION

3.1 The plasmid Design:

The cDNA sequence of the variable fragment of the light chain (V_L) and heavy chain (V_H) of antibody against the mouse Transferrin receptor in the mouse 8D3 were obtained from Boado et.al.[13] The flexible linker was formed using Glycine and Serine residues in order to conjugate the V_L, and V_H, of 8D3 antibody forming the single

binding domain of the antibody, scFv8D3. The linker was constructed as the sequence of $(Gly\text{-}Gly\text{-}Gly\text{-}Gly\text{-}Ser)_n$ with the variance of the number of n to achieve the desired length of the linker. In this case, the length of 20 amino acids was chosen to connect the V_L8D3-and-V_H8D3 domains of the antibody and a separate linker of 10 amino acids was used to join the vMIP-II to scFv8D3. The length of 20 residues was chosen to prevent the dimerization of scFv8D3.[15] Glycine and Serine are used to increase the flexibility of the linker due to the fact that Glycine only contains hydrogen as the side chain and with its small size allows the mobility of the two components of the recombinant protein.[15] Serine has the hydroxyl group side chain and will facilitate the solubility of the protein in solution by forming hydrogen bonds with the water molecules, and therefore reduces the unfavorable interaction between the linker and the protein moieties.[15] The flexibility of the linker increases the accessibility of the antibody for binding to its epitope and also increases the mobility of the vMIP-II moiety connected to the scFv8D3 fragment.

scFv8D3 expressed in pET32a was constructed with the His-tag and S-tag followed by the EK cleavage site immediately prior to the scFv8D3 N-terminus. The His-tag binds tightly to the Ni chelating column, and the 6xHis-tagged scFv8D3 can be selectively purified using high imidazole gradients. High concentration of Imidazole can efficiently deplete the binding of His-tag to the Ni beads. As shown in lane 3 of Figure 3, the protein 6xHis-scFv8D3 is expressed at the expected molecular weight of 31 kDa. As scFv8D3 is a heterogeneous gene, difficulty was encountered during expression in *E.coli* due to the low usage frequency of existing codons in the gene originating from different species.[16,17,18] Even after the protein was codon-optimized for expression in *E.coli*, low expression was observed, which was attributed to the inability

of the BL21 cells to translate the codons with rare usage in *E.coli*.[16,18] Moreover, the overexpression of the recombinant protein can lead to high toxicity of the protein to the host bacteria cells and inhibit cell growth.[16,17,18] Without the solubility fusion tag, the protein could not be expressed in sufficient quantities for purification; low expression of the protein, scFv8D3, was observed after induction for 5 hours with 1mM IPTG (Figure 3 a, lane 3).

The protein Sumo-vL10s was expressed in pET28a with the solubility fusion Sumo tag at the N-terminus of the chimeric protein. The Sumo fusion tag contains a 6xHis tag at its N-terminus and serves as the affinity tag to Ni-NTA used to purify the fusion protein. In addition to improving solubility, the Sumo tag also promotes the correct folding and structural stability of its partner protein.[19] In addition, the Sumo tag can only be cleaved off by the protease ULP-1, which recognizes the tertiary structure of the Sumo protein.[20] This can be used as a qualitative indicator for the folding of the whole recombinant protein. Moreover, ULP-1 cleaves specifically at Sumo's C- terminus at the conserved Gly-Gly motif without any extra residues at the N terminus of the protein of interest.[19,20] With the presence of Sumo, the expression of Sumo-vL10s was enhanced, and the overexpression of the fusion protein was observed on the SDS-PAGE gels after induction at 22°C for 16 hours (Figure 3b, lane 3). The expected molecular weight of Sumo-vL10s is 48.6 kDa.

a) b)

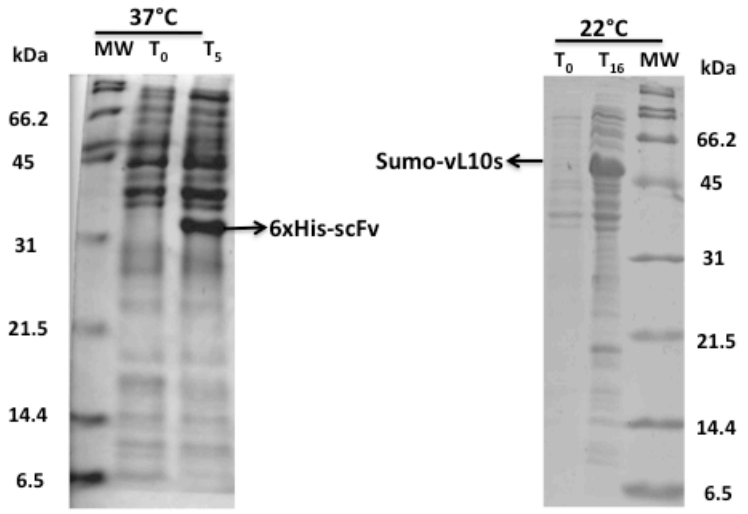

Figure 3 a: The expression of 6xHis-scFv8D3-pET32a at 37 °C. Lane 1: Broad range molecular weight marker. Lane 2: The time point of 6xHis-scFv8D3-pET32a before induction. Lane 3b: The time point of 6xHis-scFv8D3-pET32a 5 hours after induction with 1 mM IPTG. Figure 3b: The expression of Sumo-vMIPII-L-scFv8D3-pET28a in BL21 (DE3) cells at 22 °C. Lane 1: Broad range molecular weight marker. Lane 2: The time point of Sumo-vMIPII-L-scFv8D3-pET28a before induction. Lane 3: The time point of Sumo-vMIPII-L-scFv8D3-pET28a 16 hours after induction with 1 mM IPTG. Strong expression of vMIP-II-L-scFv8D3 is denoted by the arrow at the appropriate molecular weight.

3.2 Aggregate formation and inclusion body of the expression of 6xHis-scFv and Sumo-vL10s:

Both scFv8D3 and SumovL10s contains multiple disulfide bonds that are crucial to their folding and stability. Thus, formation of wrong disulfide bonds can lead to protein misfolding and aggregation into inclusion bodies. For recombinant

protein inserted into *E.coli* host cells, the disulfide bonds are ideally formed when the cysteine is oxidized in the periplasm of *E.coli*.[16,21,14,22] Due to the limited space of the periplasm of *E.coli* and over-production of desired protein, most of the disulfide bonds in the nascent protein can not be correctly formed and sent to cytoplasm of the protein.[22,23] The high reducing environment of the cytoplasm (where the expressed protein is located) prevents the formation of the disulfide bonds, causing misfolding of the proteins and formation of inclusion bodies. Comparison of Lane 2 and 3 of Figure 4 a and 4 b shows more than 95% of both proteins remain in the insoluble fraction (pellet) of the cell lysate after rupturing the cells suspended in high salt buffer. The harvested cell mass was suspended in a high concentration of NaCl (500 mM). The high salt concentration disrupts ionic bonding and the hydrogen bonds of the proteins to the solution, facilitating the protein to aggregate into the pellet (Figure 4a, lanes 3 and 4). This is sometimes desirable in order to gather all recombinant protein in one pellet as opposed to having a portion of the protein in the soluble fraction, where it must be purified separately. The proteins were then completely unfolded and solubilized using a high concentration of denaturant 6M Gnd-HCl (Figure 4a and 4b, lane 5). The protein solutions were also reduced using the reducing agent β-mercaptoethanol (βME) to break any incorrect disulfide bonds formed prior to the refolding process. The fractions of soluble and aggregated protein were separated from the cell debris by high-speed centrifugation at 4°C to prevent the over-activity of

proteases (Figures 4 a and 4 b, lanes 2,3). Inclusion bodies, due to their high density in comparison to other cellular components can be isolated from the whole cell lysate by centrifugation.

a) b)

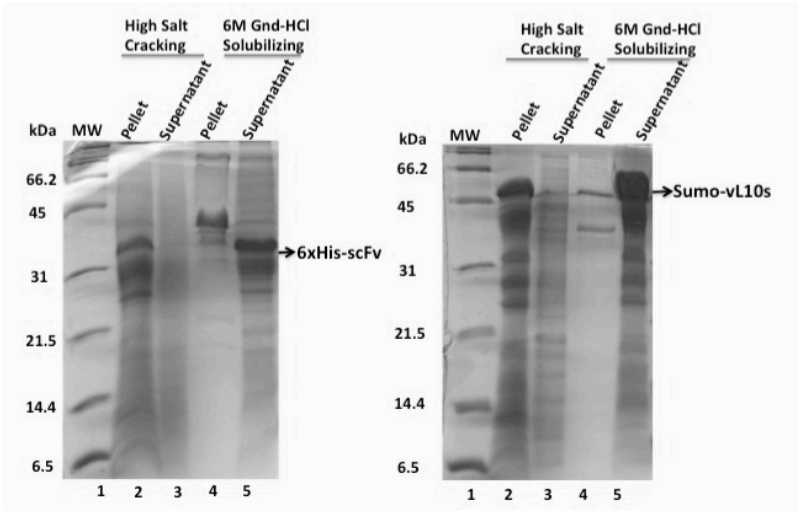

Figure 4 a: Purification of 6xHis-scFv8D3-pET32a: Lane 1: Broad range molecular weight marker. Lane 2,3: protein in supernatant (lane 2) and in the pellet (lane 3) after harvest of 6xHis-scFv8D3-pET32a in high salt cracking buffer. Lane 4: Pellet of cell lysate after solubilizing the crude pellet in 6M guanidine . Lane 5: Supernatant obtained after solubilizing the crude pellet in 6M guanidine.

Figure 4 b: Purification of Sumo-vMIPII-L-scFv8D3-pET28a: Lane 1: Broad range molecular weight marker. Lane 1: Broad range molecular weight marker. Lane 2,3: protein in supernatant (lane 2) and in the pellet (lane 3) after harvest of Sumo-vMIPII-L-scFv8D3-pET28a in high salt cracking buffer. Lane 4: Pellet of cell lysate after solubilizing the crude pellet in 6M guanidine . Lane 5: Supernatant obtained after

solubilizing the crude pellet in 6M guanidine. TCA precipitation was performed to remove guanidine chloride for preparation of gel samples.

3.3 Refolding of 6xHis-scFv8D3 and SumovL10s by stepwise dialysis with Gnd-HCl gradient:

The crude supernatant contained most of unfolded scFv8D3 and Sumo-vL10s with reduced cysteinyl residues. The target protein together with high molecular weight contaminant proteins from *E. coli* was directly refolded using a serial dialysis method to slowly removing the denaturants and introducing an oxidizing agent to enable the formation of correct disulfide bonds.[14]

Both scFv8D3 and Sumo-vL10s were refolded using the stepwise dialysis method described in Umetsu et al.[14] In this method, the concentration of the denaturant Gnd-HCl is removed slowly and additives (Arginine and oxidized glutathione, GSSG) were introduced at specific stage of dialysis to promote the formation of native disulfide bonds in the proteins. Figure 3 a and 4 a confirms the presence of scFv8D3 and Sumo-vL10s in the soluble fractions of the refolding protein solution throughout the dialysis stages from 6→3→2→1→0.5 M Guanidine-HCl. Abundant bands at approximately 31 kDa corresponding to the size of 6xHisscFv8D3 (Figure 4 a) and those between 45 and 66 kDa correspond to the size of Sumo-vL10s (Figure 4 b) were observed in the soluble protein fractions at each dialysis stage. It is worth noting that the crude protein solutions contain mostly the inactive form of scFv8D3 and Sumo-vL10s as well was other contaminant proteins, and these crude protein solutions were directly refolded before the first purification by the Ni-NTA column. Besides the recombinant protein, inclusion

bodies could also contain components from bacterial membrane, other host proteins and RNA. Therefore, the other bands besides the band of the target protein also observed on the SDS-PAGE gels likely correspond to these contaminants. The standard refolding method was used to refold scFv8D3, whereas several modifications were employed to improve the folding of Sumo-vMIPL10s. An extra dialysis step at 0.25 M Gnd-HCl stage was added. The Native buffers were changed from 50mM Tris to 20 mM NaPi and 50 mM Arginine and 50 μM GSSG was kept in the buffer prior to the 1st Ni column. Modifications were used to refold Sumo-vL10s, and due to the unsuccessful refolding of the protein using the original standard refolding method (data not shown).

In these refolding methods, Gnd-HCl was used both as a denaturant at the high concentrations of 6 M and 3 M and as a solubilizing agent at the lower concentrations of 2, 1, 0.5 and 0.25 M Gnd-HCl. Gnd-HCl is a charged molecule and can interfere with the electrostatic interactions and especially the hydrogen bonding of the side chains of the protein with the solvent, which at high concentrations causes the protein to lose its structural stability.[14,23] The gradual removal of the denaturant Gnd-HCl and the reducing agent βME via stepwise dialysis against the 6 M, 3 M and 2 M Gnd-HCl Buffer (without βME) allows the natural oxidization to occur and facilitates the formation of disulfide bonds in Sumo-vL10s and scFv8D3. The proteins remained solubilized as the concentration of Gnd-HCl was slowly reduced. [Figure 5a and 6a] According to Umetsu et al., from the 2 M Gnd to the 1 M Gnd stage, the protein solution is at an intermediate folding state with the disulfide formed partially, but the correct disulfide bonds in scFv8D3 cannot be obtained without the addition of the oxidizing reagent GSSG.[14] The natural oxidation cannot sufficiently enhance the formation of the native intradisulfide

bonds between the beta sheet of the V_L and V_H domains of scFv8D3 and of the disulfide bonds in vMIP-II.[14] In addition, L-Arginine-HCl is introduced during the 1 M Gnd-HCl dialysis stage. L-Arginine is one of the most commonly used and most generally applicable suppressors of protein aggregation.[14,24,25] L-arginine may inhibit association between the partially folded elements so that the thiol groups were unable to approach each other. L-Arginine salt contains a long side chain, which can help prevent the association between partially folded elements so that the thiol groups are unable to approach each other and form erroneous disulfide bonds.[24] Moreover, Arginine is a derivative of Gnd-HCl and contains the Guanidinium charged group at the end of its side chain and can aid in keeping the protein soluble. GSSG is composed of two glutathione molecules linked by disulfide bonds. GSSG is used as an oxidizing agent and facilitates the formation of native disulfide in the proteins by undergoing a disulfide exchange reaction. Thus, GSSG plays the crucial role in promoting the formation of the correct disulfide bonds in the protein in the refolding process.

Extra dialysis steps at 0.25 M were employed in refolding Sumo-vL10s to allow more disulfide bonds to form correctly. The lower concentrations of Arginine (50 mM) and GSSG were kept in the refolding buffer to suppress aggregates and to permit reformation of disulfide bonds, further enabling the correct refolding of the protein.

3.4 Purification of scFv8D3 and Sumo-vL10s using Ni-NTA affinity column:

After dialyzing the protein solution against the Native buffer for 6xHisscFv8D3 and Sumo-vL10s, aggregates formed upon the complete removal of solubilizing agents and additives. These aggregates are likely the contaminant proteins from the crude protein solutions that are already present in the crude proteins solution before refolding

and the misfolded proteins. The soluble and pure protein can be collected after removing the aggregates using high speed centrifugation.

The refolded scFv8D3 and Sumo-vL10s were loaded onto the Ni-NTA column twice in order to allow the His-tagged protein to bind to Ni more effectively. Figure 5 b and 6 b show that the concentration of 250mM Imidazole was sufficient to complete the binding of 6xHis-tag to the Ni column, resulting in the elution of the target protein. The wash buffers of 20 mM and 50 mM Imidazole were effective in removing impurities off the Ni column before elution step (Figure 5b, Lane 4). The SDS –PAGE gels of the elution fractions of the 1st Ni-column confirm the 90% purity of scFv8D3 and Sumo-vL10s the proteins at this step (Figure 5b, lane 5). For Sumo-vL10s, analysis of the lane 4 and 5 of Figure 6 b shows the profound bands between 14 and 21 kDa. The size of the band is much smaller than the size of 29 kDa of actual scFv8D3 by itself or a lot larger than the size of Sumo tag or vMIP-II by themselves. The band therefore likely indicates the N-terminal degradation of the fusion protein. This assumption was confirmed on the analysis of the product of the cleavage reaction of Sumo tag from Sumo-vL10s using ULP-1. The band was smaller than the actual size of the target protein of 48.6 kDa indicating the degradation of the proteins during the refolding process (Figure 6 b, lane 4,5).

a) b)

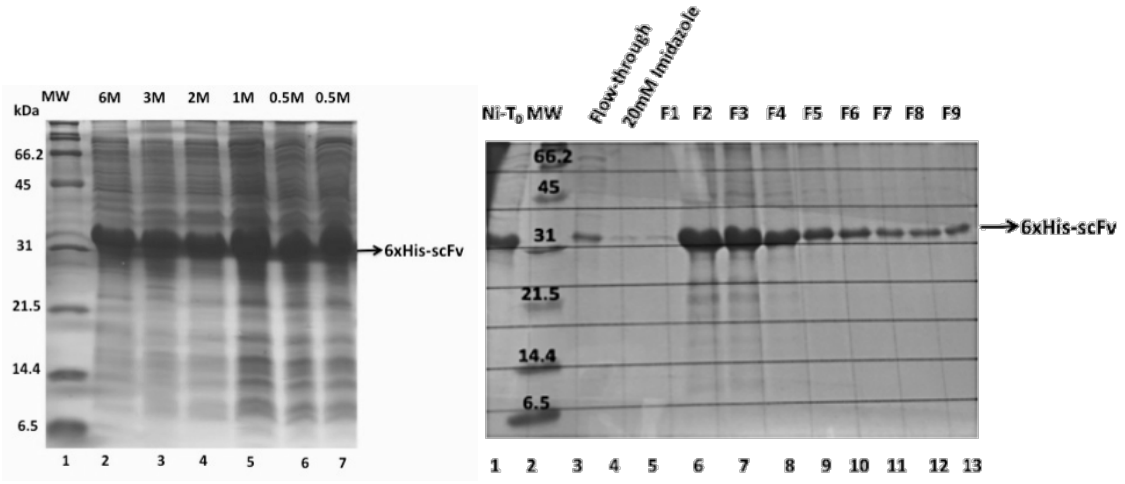

Figure 5 a: Refolding protein 6xHis-scFv8D3 using Guanidine-HCl gradient dialysis. Lane1: Broad Range Molecular Weight Marker. Lanes 2-7: The soluble fractions of the protein solution dialyzed against 6→3→2→1→0.5 M Guanidine-HCl refolding buffer. Lane 8: The protein solution in Native Buffer with free of denaturants and additive before purifying using Ni column. TCA precipitation was performed to remove guanidine chloride for preparation of gel samples.

Figure 5 b: Eluted fractions of 6xHis-scFv8D3 from Ni-NTA column using high Imidazole concentration Elution Buffer (200 mM NaCl, 50 mM Tris, pH = 7.5). Lane 1: The protein fraction prior to loading onto Ni column. Lane 2: The flow through after passing the protein solution onto Ni column twice. Lane 3: The wash fractions of 20mM Imidazole Wash Buffer. Lanes 5-15: The elution fraction of the protein solution in Elution Buffer.

a) b)

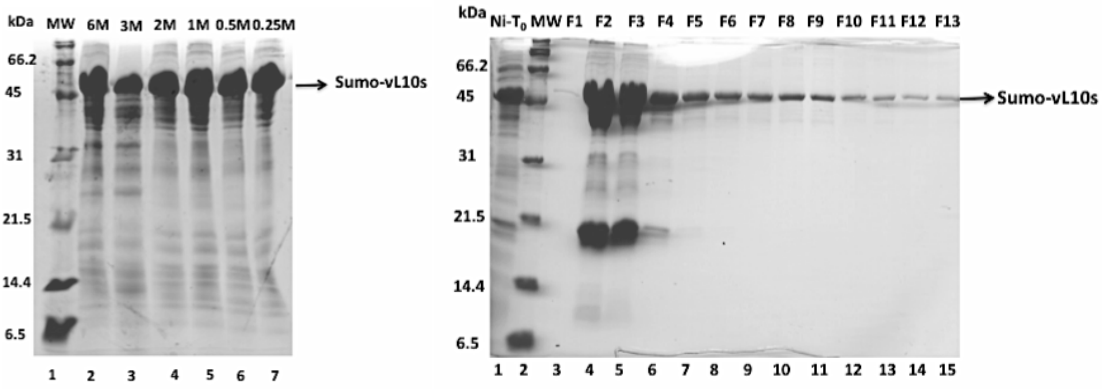

Figure 6 a: Refolding protein Sumo-vMIPII-L-scFv8D3-pET28a using Guanidine-HCl gradient dialysis. Lane1: Broad Range Molecular Weight Marker. Lane 2-7: The soluble fractions of the protein solution dialyzed against 6→3→2→1→0.5→0.25 M Guanidine-HCl refolding buffer. Lane 8: The protein solution in Native Buffer with free of denaturants and additive before purification using Ni column. The gel samples were prepared using TCA precipitation to remove Guanidine- HCl.

Figure 6 b: Eluted fractions of Sumo-vMIPII-L-scFv8D3 from Ni-NTA column using high Imidazole concentration Elution Buffer (200 mM NaCl, 250 mM Imidazole, 20 mM NaPi, pH= 7.5). Lane 1: The protein fraction prior to loading onto Ni column. Lane 2: Molecular Weight Marker. Lane 3-15: The elution fractions of the protein solution in Elution Buffer were collected in 3mL fractions.

3.5 Cutting reaction of Sumo-vL10s by ULP-1 to yield native vMIPII-L-scFv8D3:

All of the elution fractions of Sumo-vL10s were combined and dialyzed against 200 mM NaCl and 20 mM NaPi (pH= 7.5) to remove imidazole from the protein solution. Four buffer exchanges of 1L each were carried out at 4 °C and the cutting reaction with ULP-1 were initiated at the 3rd buffer exchange.

Imidazole does not affect the activity of ULP-1. The SDS-PAGE gel analysis confirms the efficient cleavage of Sumo tag. The vMIP-II-L-scFv8D3 that is free of the Sumo tag was observed at the size of approximately 35 kDa (Figure 7b, lane 3). If ULP-1 actively cleaved the sumo-vL10s, there would be 3 lanes on the SDS gels corresponding to the cut vMIP-II-L-scFv8D3 at the size of approximately 35 kDa and the cleaved Sumo tag at 13 kDa (Figure 7b, lanes 3,4,5) Sumo tends to run higher than its expected size on SDS-PAGE gels. After 5 hours, more than 90% of the protein was free of Sumo tag. This indicated that the protein could be folded correctly. Upon the removal of Sumo fusion tag using ULP-1, the free vMIP-II-L-scFv8D3 no longer has the Histidine tag and could not bind to the Ni-NTA column. The Sumo tag and uncut Sumo-vL10s are expected to bind tightly to the Ni-NTA column. Thus, isolated vMIP-II-L-scFv8D3 was obtained in the flow-through (FT) after passing the protein solution through a Ni column. The cut protein solution was passed through the Ni column twice to ensure maximal binding of the cleaved-Sumo tag and uncut Sumo-vL10s to the Ni column and the target protein can be collected as the FT from the Ni column.

From the result of SDS-PAGE gel, approximately 90% of pure vMIP-II-L-scFv8D3 was purified without any contamination of Sumo tag or uncut fusion protein (Figure 7b, lane 7).

a) b)

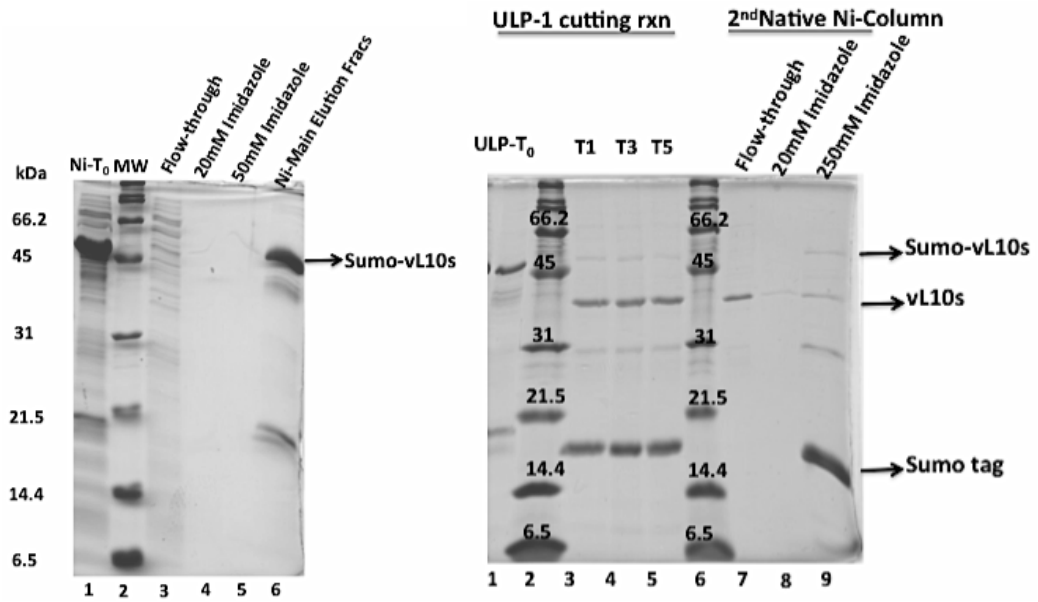

Figure 7 a: Purification of Sumo- vMIP-II-L-scFv8D3 by Ni-NTA column: Lane1: The protein fraction prior to loading onto Ni column. Lane2: Molecular Weight Marker. Lane 3: The flow-through after passing the protein solution onto Ni column twice. Lanes 4 and 5: The wash fractions of 20mM and 50mM Imidazole Wash Buffer. Lane 6: The combined fraction of all elution fractions of Sumo-vL10s in Elution Buffer (200 mM NaCl, 250 mM Imidazole, 20mM NaPi, pH=7.5) as observed in Figure 6b.

Figure 7 b. Cleavage reaction of the Sumo- vMIP-II-L-scFv8D3 by ULP-1 to obtain the native vMIP-II-L-scFv8D3. Lane 1: Sumo-vMIP-II-L-scFv8D3 after Ni column and before the cutting reaction. Lane 2: molecular weight marker, Lanes 3, 4, and 5: The ULP-1 cutting reaction of Sumo- vMIP-II-L-scFv8D3 after 1, 3, and 5 hours, respectively. Lane 6: molecular weight marker; Lane 7: The flow through of the 2nd Ni column showing purified, cleaved vMIP-II-L-scFv8D3, without the presence of his-tag containing former fusion partners and uncut protein. Lane 7: The wash fractions of the

2^{nd} Ni column after 15 column volume of Wash Buffer with 20 mM Imidazole. Lane 8: The High Imidazole wash of 250 mM Imidazole to confirm the tight binding of his-tag containing Sumo byproducts onto the Ni column compared to the cut vMIP-II-L-scFv8D3; these proteins bound to the column did not elute off the column at the low concentration of Imidazole.

3.6 NMR Analysis:

Figure 8 and 9 shows the ^{15}N-^{1}H correlation HSQC spectrum of 6xHis-scFv8D3 and vMIP-II-L-scFv8D3. The NMR spectrum of scFv8D3 shows some peaks exhibiting good dispersion from 9-11 ppm (^{1}H) indicating a folded protein. In a folded protein, the chemical shift of the residue depends significantly on its neighboring residues in the tertiary structure, leading to distinctive chemical shifts and the widely dispersed peaks observed in the NMR spectrum. In contrast, amides in an unfolded protein will not have a unique chemical environment and the signals will be the average of all the residues that the protein interacts with, resulting in broad peaks and peaks clustered around 8 ppm. 6xHis-scFv8D3 does contain a significant cluster of broad peaks from 7.8 to 8.4 ppm corresponding to the aggregated form of scFv8D3. Therefore, analysis of the NMR spectrum of scFv8D3 indicates the presence of both unfolded and folded population of scFv8D3 in the solution (Figure 8). As such, more optimal refolding conditions for scFv8D3 could be further investigated.

In contrast, and as the main result of this body of work, the NMR spectrum of vL10s (i.e. vMIP-L10-scFv8D3) shows well defined, dispersed peaks from 6-11 ppm

without any broad peaks at the center of spectrum, exhibiting the characteristics of well-folded protein (Figure 9).

In order to determine that both components of the fusion protein vMIP-L10-scFv8D3 are properly folded, it is useful to compare the fusion protein HSQC spectrum with that of each control, i.e. first with the scFv8D3 spectrum, then with a spectrum of vMIP-II. The overlaid NMR spectra of the vMIP-L10-scFv8D3 fusion protein and control scFv8D3 is shown in Figure 10. Despite the scFv8D3 being predominantly unfolded, its peaks in the folded region show high similarity to the positions of some of the folded peaks in the fusion protein (Figure 10). This provides strong evidence of the presence of folded scFv8D3 in the fusion protein.

The next spectra comparison is shown in Figure 11, where vMIP-II alone (blue) is overlaid with vMIP-L10-scFv8D3 (red). (In this figure for comparison, the refolded scFv is also shown in black). Unexpectedly, there are few or no clear vMIP-II peaks in the spectrum of vMIP-L10-scFv8D3. This could be due to several causes. First, the vMIP-L10-scFv8D3 may have been internally cleaved, removing the vMIP-II and leaving just the scFv portion of the protein. However, the spectrum of the fusion protein contains more peaks than the spectrum of scFv8D3, which together with the size of the purified protein band on the SDS-PAGE gel indicates the presence of vMIP-II in vMIP-L10-scFv8D3. To confirm that both components of the chimera (vMIP-II and scFv8D3) were indeed still present in the purified chimera, a mass spectrum was measured of the protein. The mass spectrum of the purified fragment of ^{15}N vMIP-II-L-scFv8D3 also confirmed the correct mass of ^{15}N vMIP-II-L-scFv8D3 of 35354 Da (Figure 13). All the collected peaks on the mass spectrum correspond to the proteins of the mass that are larger than

30000 Da. This confirms that the purified protein is not individual fragments of scFv8D3, vMIP-II or Sumo tag. We can conclude that the purified fusion protein and NMR spectrum most likely correspond to the refolded fusion protein. Overall, we conclude that we have successfully refolded vMIP-L10-scFv8D3, and that its scFv portion is likely folded correctly, while the vMIP-II portion does not spectroscopically resemble unliganded vMIP-II. Since the entire chimera appears to be fully folded (and vMIP-II has two disulfide bonds which are presumably successfully formed), it is possible that the vMIP-II portion of the chimera is interacting with either scFv or other vMIP-II subunits to alter its spectral properties without causing unfolding of the protein. Further experiments will clarify this.

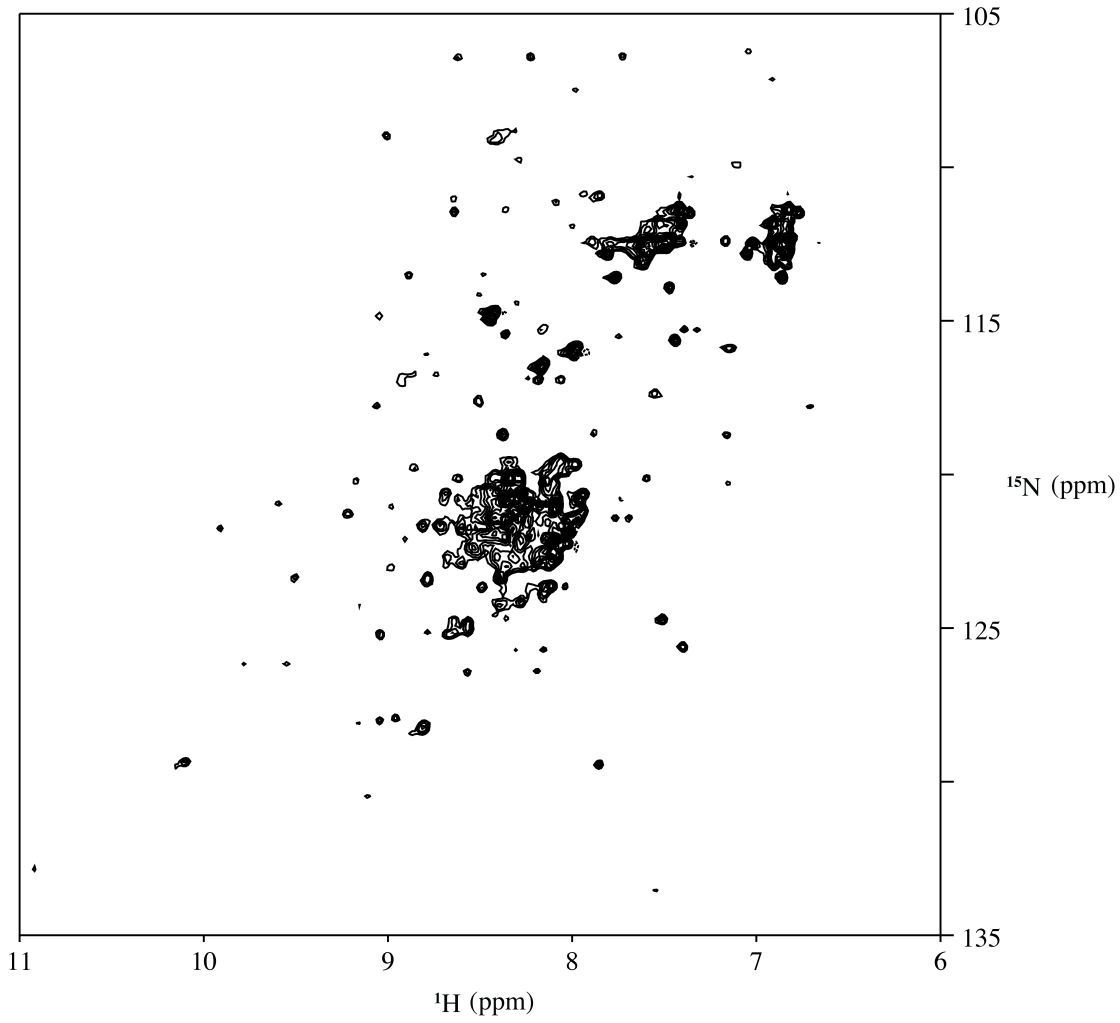

Figure 8: The ^{15}N-^{1}H HSQC NMR spectra of ^{15}N labeled 6xHis-scFv8D3 at pH=7.5

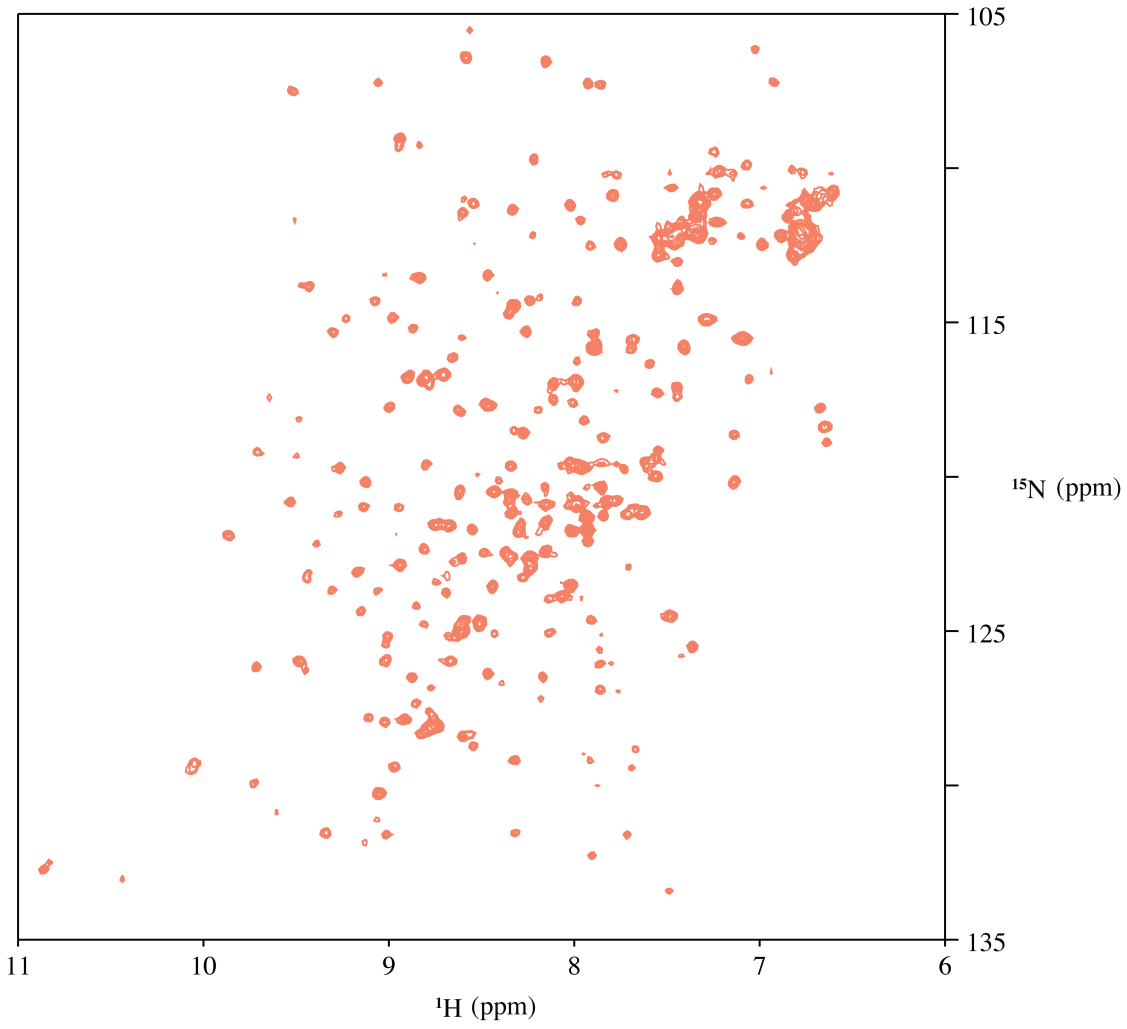

Figure 9: The ^{15}N-^{1}H HSQC spectrum of ^{15}N labeled vMIPII-L10-scFv8D3 at pH=7.5

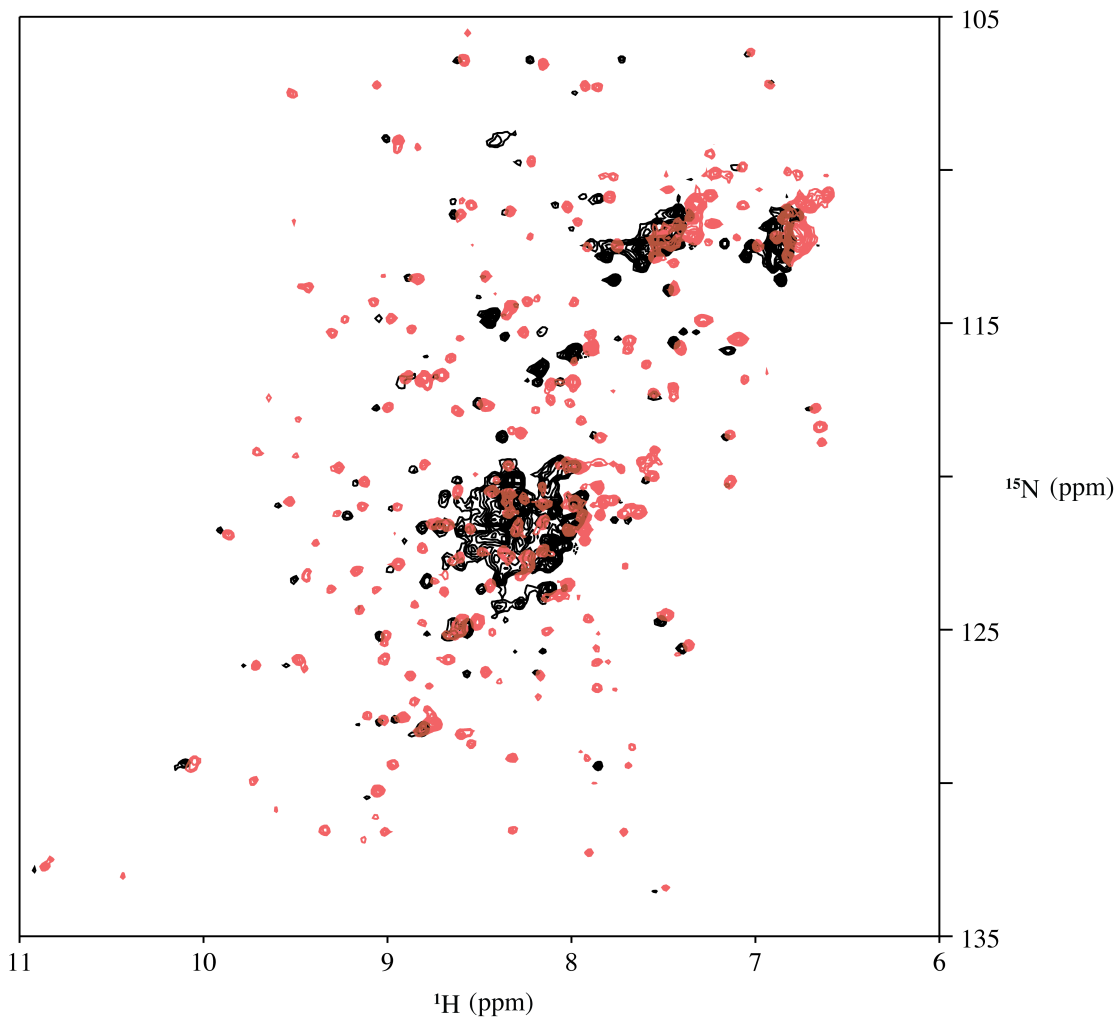

Figure 10: The Overlay ^{15}N-H HSQC NMR spectra of ^{15}N labeled vMIPII-L10-scFv8D3 (red) with the 6xHis-scFv8D3 (black) at pH=7.5

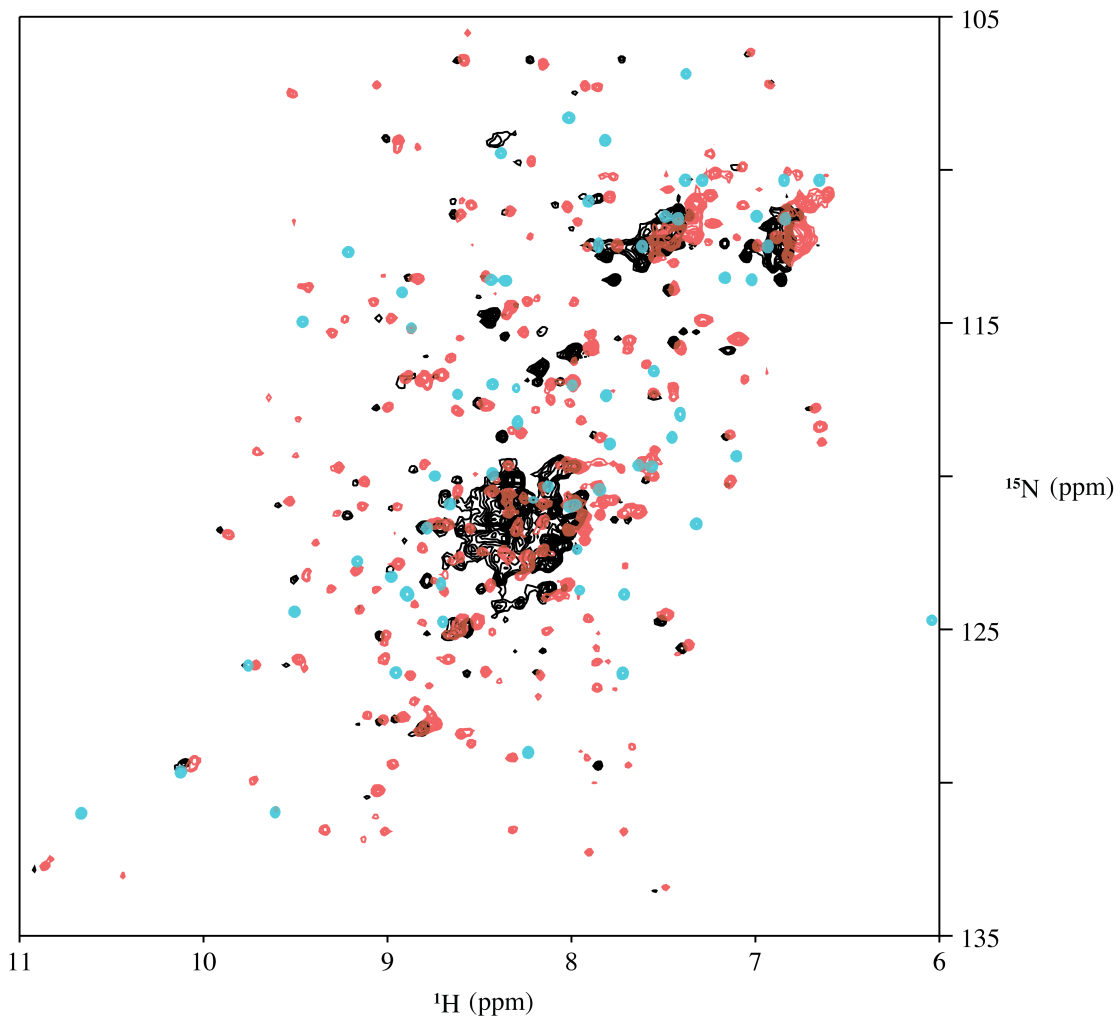

Figure 11: The overlay ^{15}N-^{1}H HSQC NMR spectra of ^{15}N labeled vMIPII-L-scFv8D3 (red) with 6xHis-scFv8D3 (black) and ^{15}NvMIP-II (light blue) adapted from Dr. Nai-Wei Kuo at pH= 7.5.[10]

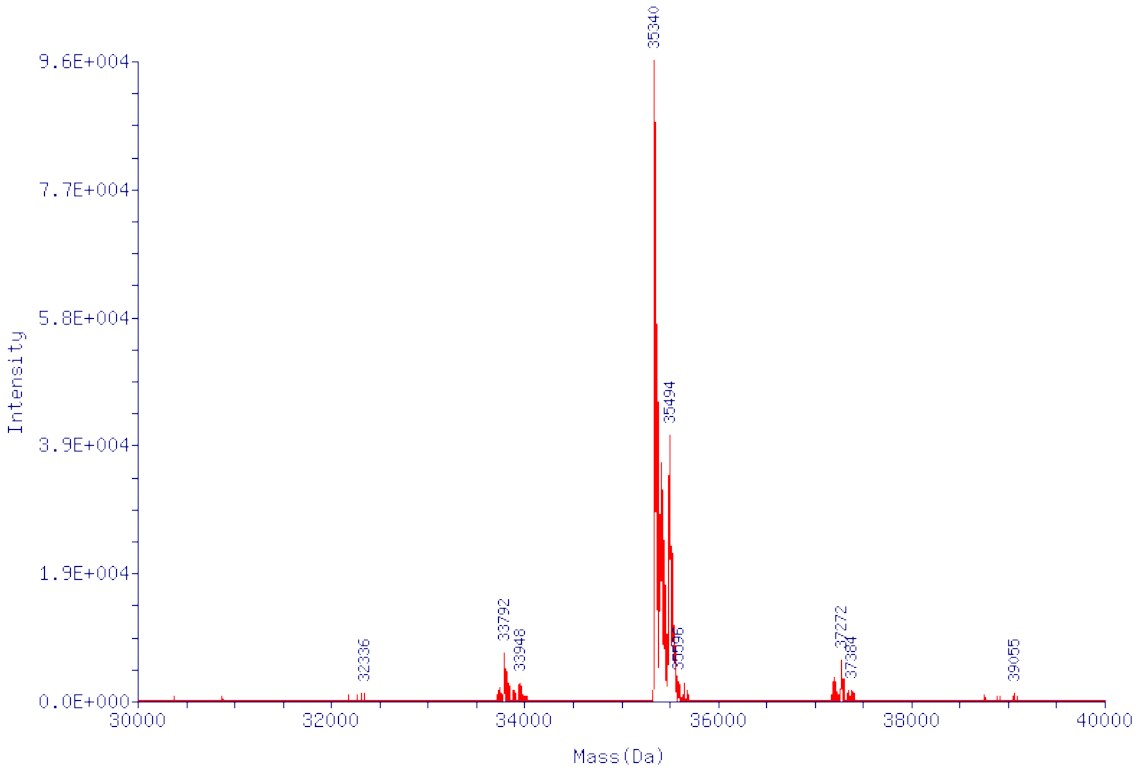

Figure 12: The deconvoluted electrospray mass spectra (ESI-MS) of ^{15}N labeled fusion protein. The expected mass of ^{15}N-labeled v vMIP-L10-scFv8D3 is 35354 Da. This spectrum provides evidence that the protein sample is indeed the desired chimera vMIP-L10-scFv8D3.

CHAPTER 4. SUMMARY AND CONCLUSIONS

4.1 Summary

The purification and refolding processes of 6xHis scFv8D3 and vMIP-II-L10-scFv8D3 were repeated twice and gave the same results. In summary, the desired proteins scFv8D3 and vMIP-II-L10-scFv8D3 were successfully designed, expressed in *E.coli*, refolded, and purified using the Gnd-HCl gradient dialysis method and Ni-NTA affinity columns. This is motivated by the potential of vMIP-II-L-scFv8D3 to serve as a potent antagonist to pro-inflammatory chemokines for treating TBI-associated inflammation in the brain. The refolding process of scFv8D3 was not as successful as the fusion protein, thus a more optimal refolding method could be investigated and developed if it is desired to produce only the scFv component of the chimera. The NMR spectrum of the vMIP-II-L10-scFv8D3 showed a nicely folded protein, indicating success with the overall goal of the project. This spectrum aligned well with the spectrum of scFv8D3 alone but, surprisingly, not with that of vMIP-II. However, several experiments provide strong evidence that the chimera has indeed been correctly produced and purified. These include the SDS-PAGE gels, the dispersed peaks in the NMR spectrum and the mass spectrum that together confirm the correct size and mass and folded state of the fusion protein. This study also demonstrates the potential to synthesize and refold a single chain variable fragment of an antibody of eukaryotic origin

utilizing a bacterial expression system. In the future, this could become a more economic and effective method of producing anti-inflammatory drugs in a form that can be shuttled to the brain and alleviate the symptoms of TBI. If the functions of vMIP-II-L10-scFv8D3 is be tested and proven, this study will uncover a way to enhance the efficacy of brain-accessible anti-inflammatory drugs to combat TBI. Various antagonists could also be conjugated to scFv8D3 and used to treat other neural degenerative diseases associated with brain inflammation. In addition, these results also demonstrate that proteins with high numbers of disulfide bonds can be refolded by implementing a step-wise dialysis with Gnd-HCl and appropriate additives such as Arginine-HCl, and oxidized/reduced Glutathione pairs. This work not only pioneers a non-invasive method to circumvent the BBB and treat brain inflammation, but it will also help to facilitate more rational designs of chemokine receptor antagonists for further research in pharmaceuticals. It introduces a new strategy to deliver anti-inflammatory drugs across the BBB by conjugating the therapeutic agents with Transferrin or the antibody that binds to Transferrin receptor, the successful realization of which would be an important breakthrough and could greatly increase the current capacity of the medical field to treat inflammation in the brain.

4.2 Future Research

The successful purification of the proteins scFv8D3 and vMIP-L10-scFv8D3 was confirmed by SDS-PAGE gels, mass spectrometry, and their folding was also confirmed by NMR spectroscopy. In order to completely elucidate the potency and mechanism of action of scFv8D3 and vMIP-L-scFv8D3, ELISA assays should be performed to validate their binding potency to TfR, and also the function of vMIP-II will be assessed as described in Niewoehner.[26] Figure 13 depicts a proposed ELISA assay to test the binding of vMIP-II-L-scFv8D3 to TfR. A 96 well plate will be coated with mouse TfR-binding domain (extracellular domain; Sino Biological) in PBS buffer at 4°C overnight. After blocking the plate with 3% BSA in PBS buffer for 1hr at room temperature, the plate will be washed 4x with Wash Buffer of 0.1% Tween-20/PBS. The purified and refolded vMIP-II-L-scFv8D3 will be added to the 96 wells-plate with the concentrations of vMIP-II-L-scFv8D3 varying between 0.01 and 150 nM in 3% BSA. The amount of 50uL of 1ug/mL of Biotinylated anti-vMIP-II antibody (R &D Systems) in blocking buffer will be added to each well for 1 hour at room temperature followed by six washes with Wash Buffer to prevent nonspecific binding of biotinylated anti-vMIP-II antibody onto the plate. 100 uL of dilute Streptavidin-HRP (R &D Systems) and 100 uL Streptavidin substrate, ABTS, will also be added for 30 minutes to detect the binding of vMIP-II-L-scFv8D3 to the extracellular TfR

binding domain coated on the plate. Upon binding of vMIP-II-L-scFv to the extracellular TfR binding domain, the ABTS will change from clear to a green color. After adding the stopping buffer, the absorbance of ABTS can be measured at 405nm and the intensity of the absorbance of ABTS will be used to quantify the concentration of the bound vMIP-II-L-scFv to the extracellular TfR binding domain. Similarly, a positive control of the ELISA assay can be carried as described above. In this control, which will show the binding ability of the scFv fragment to the transferrin receptor, the purified and refolded 6xHis-scFv will be added to the 96 well-plate after coating with mouse TfR-binding domain instead of the fusion protein. The biotinylated anti-His tag antibody will be added to detect the bind of 6xHis-scFv to the TfR binding domain. The absorbance of ABTS will be measure at 405nm and used to quantify the binding of scFv8D3 to TfR. A negative control of the ELISA assay can also be carried out with a similar setup as the actual assay to test the binding of vMIP-II-L-scFv8D3 to TfR but without the addition of vMIP-II-L-scFv8D3. Because the vMIP-II-L-scFv8D3 is not added on the plate to bind to the extracellular TfR binding domain coated on the plate, the biotinylated anti-vMIP-II antibody will not bind to the fusion protein and will be removed from the plate during excessive washing steps. This also leads to the removal of Streptavidin-HRP and no color change of ABTS. Besides the binding assay to test for the function of vMIP-II-L-scFv8D3, further studies to optimize

the refolding of scFv8D3 and the structure of vMIP-II-L-scFv8D3 should also be carried out to optimize manufacture of and gain more insights into this potent drug target.

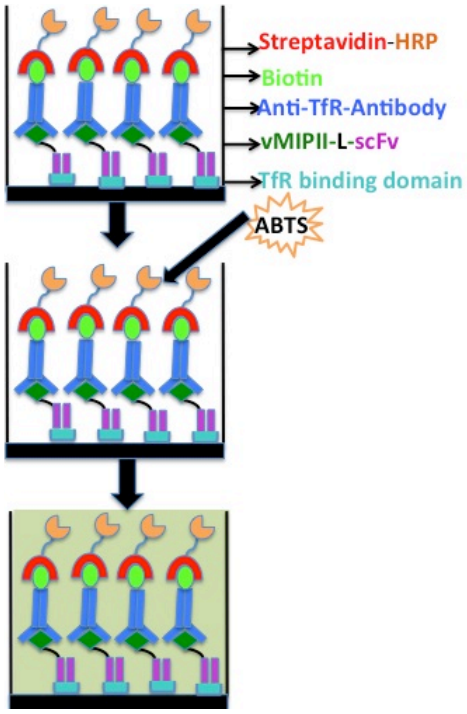

Figure 13: A possible set of ELISA experiments to test the function of vMIP-II-L-scFv8D3 in its ability to bind to the Transferrin Receptor.

REFERENCES:

1. TBI: Get the Facts | Concussion | Traumatic Brain Injury | CDC Injury Center. *Cdc.gov.* N.p., 2016. Web. 5 Dec. 2016.

2. Woodcock, T., and Morganti-Kossmann, M. C. (2013) The role of markers of inflammation in traumatic brain injury. *Front. Neurol.*

3. Abbott, N. J., Patabendige, A. A. K., Dolman, D. E. M., Yusof, S. R., and Begley, D. J. (2010) Structure and function of the blood-brain barrier. *Neurobiol. Dis. 37*, 13–25.

4. Pardridge, W. M. (2012) Drug transport across the blood-brain barrier. *J. Cereb. blood flow Metab. 32*, 1959–72.

5. Griffith, J. W., Sokol, C. L., and Luster, A. D. (2014) Chemokines and Chemokine Receptors: Positioning Cells for Host Defense and Immunity. *Annu. Rev. Immunol 32*, 659–702.

6. Charo, I. F., and Ransohoff, R. M. (2006) The Many Roles of Chemokines and Chemokine Receptors in Inflammation *6*.

7. Kufareva, I., Salanga, C. L., and Handel, T. M. (2015) Chemokine and chemokine receptor structure and interactions: implications for therapeutic strategies.

8. Liwang, A. C., Wang, Z. X., Sun, Y., Peiper, S. C., and Liwang, P. J. (1999) The solution structure of the anti-HIV chemokine vMIP-II. *Protein Sci. 8*, 2270–80.

9. Takami, S., Minami, M., Nagata, I., Namura, S., and Satoh, M. Chemokine Receptor Antagonist Peptide, Viral MIP-II, Protects the Brain Against Focal Cerebral Ischemia in Mice.

10. Liwang. (2013) A Comparison of 5P12-vMIP-II and vMIP-II as HIV-1 Entry Inhibitors. *Biochem Physiol*.

11. Macedo, M. F., and de Sousa, M. (2008) Transferrin and the transferrin receptor: of magic bullets and other concerns. *Inflamm. Allergy Drug Targets 7*, 41–52.

12. Li, J. Y., Sugimura, K., Boado, R. J., Lee, H. J., Zhang, C., Duebel, S., and Pardridge, W. M. (1999) Genetically engineered brain drug delivery vectors: cloning, expression and in vivo application of an anti-transferrin receptor single chain antibody-streptavidin fusion gene and protein. *Protein Eng. 12*, 787–96.

13. Boado, R. J., Zhang, Y., Wang, Y., and Pardridge, W. M. (2009) Engineering and expression of a chimeric transferrin receptor monoclonal antibody for blood-brain barrier delivery in the mouse. *Biotechnol. Bioeng. 102*, 1251–1258.

14. Umetsu, M., Tsumoto, K., Hara, M., Ashish, K., Goda, S., Adschiri, T., and Kumagai, I. (2003) How additives influence the refolding of immunoglobulin-folded proteins in a stepwise dialysis system: Spectroscopic evidence for highly efficient refolding of a single-chain Fv fragment. *J. Biol. Chem. 278*, 8979–8987.

15. Chen, X., Zaro, J. L., and Shen, W. C. (2013) Fusion protein linkers: Property, design and functionality. *Adv. Drug Deliv. Rev.*

16. Rosano, G. L., and Ceccarelli, E. A. (2014) Recombinant protein expression in Escherichia coli: Advances and challenges. *Front. Microbiol.*

17. Dumon-Seignovert, L., Cariot, G., and Vuillard, L. (2004) The toxicity of recombinant proteins in Escherichia coli: A comparison of overexpression in BL21(DE3), C41(DE3), and C43(DE3). *Protein Expr. Purif.*

18. Saïda, F., Uzan, M., Odaert, B., and Bontems, F. (2006) Expression of Highly Toxic Genes in E. coli: Special Strategies and Genetic Tools. *Curr. Protein Pept. Sci. 7*, 47–56.

19. Malakhov, M. P., Mattern, M. R., Malakhova, O. A., Drinker, M., Weeks, S. D., and Butt, T. R. (2004) SUMO fusions and SUMO-specific protease for efficient expression and purification of proteins. *J. Struct. Funct. Genomics 5*, 75–86.

20. Malhotra, A. (2009) Chapter 16 Tagging for Protein Expression. *Methods Enzymol.* 1st ed. Elsevier Inc.

21. Tsumoto, K., Ejima, D., Kumagai, I., and Arakawa, T. (2003) Practical considerations in refolding proteins from inclusion bodies. *Protein Expr. Purif.*

22. Popplewell, A. G., Sehdev, M., Spitali, M., Weir, a N. C., Kwong, K. Y., Rader, C., Knappik, A., Brundiers, R., Zhao, Y., Gutshall, L., Jiang, H., Baker, A., Beil, E., Obmolova, G., Carton, J., Taudte, S., and Amegadzie, B. (2009) Expression of antibody fragments by periplasmic secretion in Escherichia coli. *Methods Mol. Biol. 67*, 1929–1943.

23. Morjana, N. A., Mckeone, B. J., Gilbert, H. F., and McLean, M. (1993) Guanidine hydrochloride stabilization of a partially unfolded intermediate during the reversible denaturation of protein disulfide isomerase. *Biochemistry 90*, 2107–2111.

24. Baynes, B. M., Wang, D. I. C., and Trout, B. L. (2005) Role of arginine in the stabilization of proteins against aggregation. *Biochemistry*.

25. Lange, C., and Rudolph, R. Suppression of Protein Aggregation by L - Arginine.

26. Niewoehner, J., Bohrmann, B., Collin, L., Urich, E., Sade, H., Maier, P., Rueger, P., Stracke, J. O., Lau, W., Tissot, A. C., Loetscher, H., Ghosh, A., and Freskgård, P. O. (2014) Increased Brain Penetration and Potency of a Therapeutic Antibody Using a Monovalent Molecular Shuttle. *Neuron 81*, 49–60.

APPENDICES:

APPENDIX A: The plasmid design of Sumo-vMIP-II-L-scFvD3

- **The gene construct of pET28a vMIP-II L10 scFv8D3:**

RBS NcoI First ATG His Tag NdeI NheI SUMO vMIP-II Linker V_L8D3 Linker

V_H8D3 Stop codon SacI SalI HindIII NotI/EagI Xho1

TTTAAGAAGGAGATATACCATGGGCAGCAGCCATCATCATCATCATCACAGC

AGCGGCCTGGTGCCGCGCGGCAGCCATATGGCTAGCATGTCGGACTCAGAAG

TCAATCAAGAAGCTAAGCCAGAGGTCAAGCCAGAAGTCAAGCCTGAGACTC

ACATCAATTTAAAGGTGTCCGATGGATCTTCAGAGATCTTCTTCAAGATCAAA

AAGACCACTCCTTTAAGAAGGCTGATGGAAGCGTTCGCTAAAAGACAGGGTA

AGGAAATGGACTCCTTAAGATTCTTGTACGACGGTATTAGAATCCAAGCTGA

TCAGACCCCTGAAGATTTGGACATGGAGGATAACGATATTATTGAGGCTCAC

AGAGAACAGATTGGTGGACTTGGTGCTTCATGGCACCGTCCGGATAAATGTT

GTCTGGGCTACCAAAAACGTCCGCTGCCGCAAGTGCTGCTGAGCAGCTGGTA

TCCGACCAGCCAGCTGTGCTCTAAACCGGGCGTTATTTTTCTGACGAAACGTG

GTCGCCAGGTTTGTGCAGATAAAAGCAAAGACTGGGTCAAAAAACTGATGCA

GCAACTGCCGGTTACCGCTCGTGGTGGCGGGGGTTCGGGTGGCGGCGGTTCT

GATATCCAGATGACCCAGAGCCCGGCGTCACTGAGCGCCAGCCTGGAAGAA

ATTGTTACCATCACGTGCCAGGCATCTCAAGATATTGGCAACTGGCTGGCTTG

GTATCAGCAAAAACCGGGTAAAAGTCCGCAGCTGCTGATCTACGGCGCAACC

TCGCTGGCTGATGGTGTGCCGAGCCGTTTTTCTGGCAGTCGCTCCGGTACGCA

GTTCAGTCTGAAAATTTCCCGTGTGCAAGTTGAAGACATTGGCATCTATTACT

GCCTGCAGGCGTATAATACCCCGTGGACGTTTGGCGGTGGCACCAAACTGGA

ACTGAAACGCGGTGGCGGTGGCTCTGGTGGCGGTGGCAGTGGTGGCGGTGGC

TCCGGTGGCGGTGGCTCAGAAGTCCAGCTGGTTGAATCCGGTGGCGGTCTGG

TTCAACCGGGTAACTCACTGACCCTGTCGTGTGTCGCGAGCGGCTTTACGTTC

AGCAATTACGGTATGCATTGGATTCGTCAGGCGCCGAAGAAAGGCCTGGAAT

GGATTGCCATGATCTACTACGATAGTTCCAAAATGAACTACGCCGACACCGT

CAAAGGTCGTTTCACGATCTCTCGCGATAACAGTAAAAATACCCTGTACCTG

GAAATGAATTCACTGCGCTCGGAAGACACGGCGATGTATTACTGTGCCGTGC

CGACCTCTCATTATGTGGTTGATGTTTGGGGCCAGGGTGTTTCAGTTACCGTT

TCTTCTTAAGAGCTCCGTCGACAAGCTTGCGGCCGCACTCGAGCACCACC

- **The protein sequence of pET28a vMIP-II L10 scFv8D3:**

SUMO vMIP-II Linker V_L8D3 Linker V_H8D3

MGSSHHHHHHSSGLVPRGSHMASMSDSEVNQEAKPEVKPEVKPETHINLKVSD

GSSEIFFKIKKTTPLRRLMEAFAKRQGKEMDSLRFLYDGIRIQADQTPEDLDMED

NDIIEAHREQIGGLGASWHRPDKCCLGYQKRPLPQVLLSSWYPTSQLCSKPGVIF

LTKRGRQVCADKSKDWVKKLMQQLPVTARGGGGSGGGGSDIQMTQSPASLSAS

LEEIVTITCQASQDIGNWLAWYQQKPGKSPQLLIYGATSLADGVPSRFSGSRSGT

QFSLKISRVQVEDIGIYYCLQAYNTPWTFGGGTKLELKRGGGGSGGGGSGGGGS

GGGGSEVQLVESGGGLVQPGNSLTLSCVASGFTFSNYGMHWIRQAPKKGLEWIA

MIYYDSSKMNYADTVKGRFTISRDNSKNTLYLEMNSLRSEDTAMYYCAVPTSH

YVVDVWGQGVSVTVSS

APPENDIX B: THE PLASMID DESIGN OF 6xHis-scFvD3

- **The DNA Sequence 6xHis-scFv8D3= No Txn V_L8D3-Linker-V_H8D3 pET32a:**

T7 Promoter Lac operator RBS *NdeI* His Tag Thrombin S-Tag BglII Frame Shift **EK cut site** V_L8D3 Linker V_H8D3 **Stop codon** SacI SalI HindIII NotI/EagI Xho1 T7 Terminator

TAATACGACTCACTATAGGGGAATTGTGAGCGGATAACAATTCCCCTCTAGA

AATAATTTTGTTTAACTTTAAGAAGGAGATATA*CATATG*CACCATCATCATCA

TCATTCTTCTGGTCTGGTGCCACGCGGTTCTGGTATGAAAGAAACCGCTGCTG

CTAAATTCGAACGCCAGCACATGGACAGCCCAGATCTC**GACGATGATGACA**

AAGATATCCAGATGACCCAGAGCCCGGCGTCACTGAGCGCCAGCCTGGAAG

AAATTGTTACCATCACGTGCCAGGCATCTCAAGATATTGGCAACTGGCTGGCT

TGGTATCAGCAAAAACCGGGTAAAAGTCCGCAGCTGCTGATCTACGGCGCAA

CCTCGCTGGCTGATGGTGTGCCGAGCCGTTTTTCTGGCAGTCGCTCCGGTACG

CAGTTCAGTCTGAAAATTTCCCGTGTGCAAGTTGAAGACATTGGCATCTATTA

CTGCCTGCAGGCGTATAATACCCCGTGGACGTTTGGCGGTGGCACCAAACTG

GAACTGAAACGCGGTGGCGGTGGCTCTGGTGGCGGTGGCAGTGGTGGCGGTG

GCTCCGGTGGCGGTGGCTCAGAAGTCCAGCTGGTTGAATCCGGTGGCGGTCT

GGTTCAACCGGGTAACTCACTGACCCTGTCGTGTGTCGCGAGCGGCTTTACGT

TCAGCAATTACGGTATGCATTGGATTCGTCAGGCGCCGAAGAAAGGCCTGGA

ATGGATTGCCATGATCTACTACGATAGTTCCAAAATGAACTACGCCGACACC
GTCAAAGGTCGTTTCACGATCTCTCGCGATAACAGTAAAAATACCCTGTACCT
GGAAATGAATTCACTGCGCTCGGAAGACACGGCGATGTATTACTGTGCCGTG
CCGACCTCTCATTATGTGGTTGATGTTTGGGGCCAGGGTGTTTCAGTTACCGT
TTCTTCT**TAA**GAGCTCCGTCGACAAGCTTGCGGCCGCACTCGAGCACCACCA
CCACCACCACTGAGATCCGGCTGCTAACAAAGCCCGAAAGGAAGCTGAGTTG
GCTGCTGCCACCGCTGAGCAATAACTAGC

- **The protein sequence of 6xHis-scFv8D3= 6xHis-V_L8D3-Linker-V_H8D3 protein sequence:**

His Tag Thrombin S-Tag **EK cut site** V_L8D3 Linker V_H8D3

MHHHHHHSSGLVPRGSGMKETAAAKFERQHMDSPDLDDDDKDIQMTQSPASLS
ASLEEIVTITCQASQDIGNWLAWYQQKPGKSPQLLIYGATSLADGVPSRFSGSRS
GTQFSLKISRVQVEDIGIYYCLQAYNTPWTFGGGTKLELKRGGGGSGGGGSGGG
GSGGGGSEVQLVESGGGLVQPGNSLTLSCVASGFTFSNYGMHWIRQAPKKGLE
WIAMIYYDSSKMNYADTVKGRFTISRDNSKNTLYLEMNSLRSEDTAMYYCAVP
TSHYVVDVWGQGVSVTVSS